

Progressive neuronal loss and behavioral impairments of transgenic C57BL/6 inbred mice expressing the carboxy terminus of amyloid precursor protein

Kang-Woo Lee,^{a,b} Joo-Young Im,^{a,b} Jin-Sook Song,^c Si Hyoung Lee,^a Ho-Jeong Lee,^a Hye-Yeong Ha,^a Jae-Young Koh,^d Byoung Joo Gwag,^e Sung-Don Yang,^c Sang-Gi Paik,^b and Pyung-Lim Han^{a,*}

^aDepartment of Neuroscience, Neuroscience Research Center and Medical Research Institute, Ewha Womans University School of Medicine, 911-1 Mok-6-Dong, Yangchun-Gu, Seoul 158-710, South Korea

^bDepartment of Biology, Chungnam National University, Daejeon, South Korea

^cDivision of Biomedical Sciences, KRICT, Daejeon, South Korea

^dDepartment of Neurology, National Creative Research Initiative Center for the Study of CNS Zinc, University of Ulsan College of Medicine, Seoul, South Korea

^eDepartment of Pharmacology, Ajou University School of Medicine, Suwon, South Korea

Received 23 September 2004; revised 23 September 2005; accepted 27 September 2005
Available online 11 November 2005

The β -secretase cleaved A β -bearing carboxy-terminal fragments (β CTFs) of amyloid precursor protein (APP) in neural cells have been suggested to be cytotoxic. However, the functional significance of β CTFs in vivo remains elusive. We created a transgenic mouse line Tg- β CTF99/B6 expressing the human β CTF99 in the brain of inbred C57BL/6 strain. Tg- β CTF99/B6 mouse brain at 12–16 months showed severely down-regulated calbindin, phospho-CREB, and Bcl-x_L expression and up-regulated phospho-JNK, Bcl-2, and Bax expression. Neuronal cell density in the Tg- β CTF99/B6 cerebral cortex at 16–18 months was lower than that of the non-transgenic control, but not at 5 months. At 11–14 months, Tg- β CTF99/B6 mice displayed cognitive impairments and increased anxiety, which were not observed at 5 months. These results suggest that increased β CTF99 expression is highly detrimental to the aging brain and that it produces a progressive and age-dependent AD-like pathogenesis.

© 2005 Elsevier Inc. All rights reserved.

Keywords: AD model; CTF; Neuronal loss; Cognitive deficits; Transgenic animal

Introduction

Proteolytic cleavages of APP generate multiple forms of C-terminal fragments (CTFs): β -amyloid peptide (A β) can be produced by sequential action of β - and γ -secretases (Steiner et al., 1999). A β -bearing carboxy-terminal fragments (β CTFs) can be produced by β -secretase (Suh and Checler, 2002). Amyloid intracellular domain or AICD (CTF57 and CTF59) can be produced by γ -secretase (Yu et al., 2001a; Suh and Checler, 2002). CTF31 can be produced by caspases (Gervais et al., 1999; Lu et al., 2000). Increased production of β -amyloid peptide (A β) has been thought to be involved in the pathogenesis of Alzheimer's disease (AD) (Steiner et al., 1999). Recent studies have postulated that β CTFs or other C-terminal fragments also play a role in AD-related pathogenesis (Suh and Checler, 2002), although the precise roles of these fragments in AD remain yet to be explored.

Presenilin-1 (PS1) may be a key component of γ -secretase complex. PS1 has been considered to be a therapeutic target for the treatment and the delayed expression of AD symptoms (Li et al., 2000; Esler and Wolfe, 2001). The PS1-deficient mice generated by the conventional knockout strategy were embryonic lethal (Wong et al., 1997). However, recent studies with a conditional knockout strategy have circumvented the lethality of PS1-deficient mice and generated adult animals lacking PS1 specifically in the brain (Yu et al., 2001b; Dewachter et al., 2002). The study involving these double transgenic mice carrying both the PS1 conditional mutation and the APP_{V717I} transgene revealed that the elimination of the γ -secretase activity provided by PS1 markedly reduced A β production, plaque deposition, and rescued impaired

* Corresponding author. Fax: +82 2 2653 8891.

E-mail address: plhan@ewha.ac.kr (P.-L. Han).

Available online on ScienceDirect (www.sciencedirect.com).

hippocampal LTP but that it did not correct the deficits in learning that APP_{V717F} transgenic mice displayed (Dewachter et al., 2002). Although the underlying mechanism has not yet been clearly elucidated, these studies show that the loss of γ -secretase activity in the brain leads to the severe accumulation of β CTF99 and raises the possibility that β CTF99 accumulation might cause cognitive deficits in the absence of plaque deposition in their double transgenic mice. It also raises the question as to whether other biochemical impairments or behavioral alterations present in APP_{V717F} transgene mice can be reverted in their double transgenic mice. Regarding that PS1 has pleiotropic roles in brain cell functions, e.g., Notch (Naruse et al., 1998; Song et al., 1999) and N-cadherin (Marambaud et al., 2003) processing, it needs to be answered whether the observed learning deficits of the conditional PS1 knockout mice used in their studies were produced solely by β CTF99, by other PS1-cleaved products, or by the lack of a PS1-dependent physiology.

More direct evidence for the *in vivo* role of β CTF99 is to be ascertained from studies with transgenic mice expressing β CTF99 in the brain. To date, nine research groups have independently created transgenic mouse lines expressing various CTF forms of the human APP in the brain. Five of these lines showed either neuronal atrophy (Neve et al., 1996; Oster-Granite et al., 1996; Nalbantoglu et al., 1997; Sato et al., 1997) or impaired learning (Nalbantoglu et al., 1997; Berger-Sweeney et al., 1999; Lalonde et al., 2002a) at age 12–28 months, whereas the other four lines including the recent reported one did not display any obvious neuronal loss or cognitive impairment (Shoji et al., 1990; Sandhu et al., 1991; Araki et al., 1994; Sberna et al., 1998; Li et al., 1999; Rutten et al., 2003). Thus, the developed transgenic mice expressing CTFs showed conflicting results that ranged from no phenotype to AD-like pathogenesis. Accordingly, the *in vivo* role of β CTF99 remains elusive. All CTF-expressing transgenic lines developed thus far were created from compound genetic backgrounds, such as the C57BL/6–DBA/2 hybrids (Li et al., 1999; Rutten et al., 2003), the C57BL/6–SJL hybrids (Kammesheidt et al., 1992; Fukuchi et al., 1996; Oster-Granite et al., 1996), or the C3H–C57BL/6 hybrids (Nalbantoglu et al., 1997; Sato et al., 1997). It is not clear whether these complex genetic backgrounds contribute to the conflicting results on the *in vivo* role of β CTF99 or the difference in the design of transgenic cassettes including the choices of promoters and the specific sequences of the transgene itself is involved.

The current study was undertaken to evaluate the role of β CTF99 in the pathophysiology of the aging brain, using a newly generated transgenic mouse line expressing β CTF99 in inbred C57BL/6 mice. We found that the transgenic expression of β CTF99(V717F) is highly toxic to the aging brain and results in the progressive and age-dependent expression of the biochemical markers of AD, in combination with neuronal loss, and impaired psychiatric and cognitive behaviors.

Materials and methods

Generation of β CTF99 transgenic mice

The cloning of the human APP cDNA sequence has been described recently (Lee et al., 2004). The cDNA sequence for β CTF99 carrying the V717F mutation of APP751 was produced by a PCR method using the second half of APP751 cDNA as a template and the primer sets of app-sig-f (5'-CGATTTAGATCTTGACGGG-

GAAAG-3'), app-sig-r (5'-CGGAATTCTGCATCCGCCCGAGC-CGTCCAGGCGGC-3'). Here, V717F in β CTF99(V717F) represents the Indiana mutation described previously (Lee et al., 2004). The resulting product was subcloned into the *Bam*HI/*Eco*RI site of pBluscript II, which was used for another PCR using the primers of app-koz-f (5'-GCTCTAGACCATGCTGCCCGGTTTGGCACTGCTC-3'), app-koz-r (5'-CCC GCGCGGCGGCCGCTTCATTAATG-3'). After digesting with *Eco*RI, the resulting product was fused to the β CTF cDNA to translate the signal peptide and β CTF fusion protein. To increase the translation efficiency, we introduced the Kozak sequence (GACC) in front of the ATG codon of the signal sequence. The V717F mutation of APP751 was introduced by PCR using two primers of app-717-f (5'-GCGA-CAGTGATCTTCATCACCTTG-3') and app-1r (5'-GGGGGAC-TAGTTCTGCATCTGCTC-3').

The intron B of human β globin gene was amplified by PCR using the primers of hglob-f (5'-GATCCTGAGAACTTCAGG-3') and hglob-r (5'-TCTTTGCCAAAGTGATGG-3') and genomic DNA, which was obtained from the human neuroblastoma cell line SH-SY5Y, as a template. The resulting 918 bp fragment was inserted between the PDGF- β promoter and the β CTF99(V717F) cDNA. The SV40 late polyadenylation sequence (247 bp) was prepared from pGK-neo-pA (Lee et al., 2002). The PDGF- β gene promoter (1.2 kb) was a gift from Dr. Tucker Collins (Harvard Medical School, USA). Finally, PDGF- β CTF99(V717F)-pA and PDGF- β -intron- β CTF99(V717F)-pA were constructed. The APP signal sequence and mutation in β CTF99(V717F) were confirmed by DNA sequencing. Each of the purified linearized transgenic constructs was microinjected into the pronuclei of fertilized eggs prepared from inbred C57BL/6 mice (Korea Research Institute of Chemical Technology, Daejeon, Korea). The injected eggs were transferred to the oviduct of pseudopregnant female (ICR) mice by following a standard method (Horgan et al., 1994).

The transgenic lines were determined by genomic Southern blot and PCR methods. Blots carrying 15 μ g per lane of *Spe*I-digested genomic DNA were hybridized with a ³²P-labeled probe prepared from the 350 bp *Spe*I fragment at the C-terminus of APP cDNA (Fig. 1A). The PCR primers used were trapp-fs (5'-GCTTGATATCGAATTCCTGCAGC-3') and trapp-r1 (5'-ATGTATCTTATCATGTCTGGACCG-3') for the amplification of β CTF99 (-intron), trint-fl (5'-AATGTATCATGCCTCTTTGCACC-3'), a n d s v 4 0 p A - r 1 (5'-GTTTCGAGCTCATAATCAGCCATACCACATTTG-3') for the amplification of β CTF99. The transgenic mice lines were maintained by crossing with C57BL/6 inbred mice. The transgenic mice used in this study were heterozygous with respect to the transgene.

Northern blot analysis

Northern blot analysis was performed as previously described (Lee et al., 2004). To be brief, a membrane blot carrying 30 μ g of total RNA was prepared after separating on denaturing agarose gel (1% agarose, 6.2% formaldehyde in 0.5 \times MOPS) and hybridized with a ³²P-labeled probe prepared from the *Spe*I-digested fragment (350 bp) of β CTF99 (Fig. 1B).

Western blot analysis and histological works

Western blot analysis and immunostaining were performed as previously described (Che et al., 2001). For the Western blot analysis, mouse brain tissue was homogenized in 4°C lysis buffer

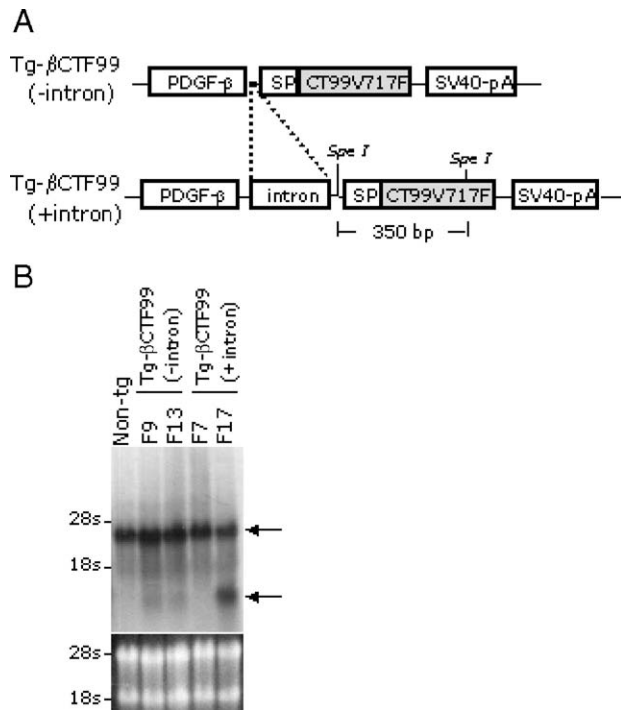


Fig. 1. Generation of transgenic mice expressing β CTF99 in the brain. (A) The transgenic cassette PDGF- β CTF99-pA (top) contained PDGF- β promoter, APP signal peptide (SP), the A β containing C-terminal 99 amino acids of APP with the V71F mutation and the SV40 polyadenylation sequence (SV40-pA). PDGF-intron- β CTF99-pA (bottom) included the intron derived from the human β -globin gene. (B) Northern blot probed with the C-terminal *SpeI* fragment detected an endogenous APP transcript of \sim 3.5 kb and a transgene-derived transcript of \sim 700 bp (arrows). The β CTF99-#F17 line showed highest transgene expression, which was greater than the level of endogenous APP.

(50 mM Tris, pH 8.0, 150 mM NaCl, 1% NP-40, 0.1% SDS, 0.5% sodium deoxycholate) containing 1 mM phenylmethylsulfonyl fluoride and protease inhibitor (CompleteTM; Roche, Mannheim, Germany). Each lane was loaded with 30 μ g protein. The separated proteins were transferred onto a PVDF membrane (Bio-Rad, Hercules, CA, USA), and the membranes were blocked with 5% non-fat dry milk, 2% BSA, 4% FBS, 4% horse serum, 4% goat serum in Tris-buffered saline, and 0.1% Tween 20. Immunoblots were detected using ECL detection reagents (Santa Cruz, CA, USA).

For the detection of β CTF99, the brain tissues were homogenized in 1:10 (g/vol) Tris-buffered saline (TBS) containing 50 mM Tris-HCl (pH 8.0), 175 mM NaCl, 5 mM EDTA, 2 mM phenylmethylsulfonyl fluoride, and a protease inhibitor cocktail (CompleteTM; Roche, Mannheim, Germany). Fifty micrograms of the protein sample were mixed with an equal volume of 2 \times Laemmli sample buffer containing 10% β -mercaptoethanol, boiled for 10 min, and then electrophoresed on 16.5% Tris/tricine agarose gel as described (Marambaud et al., 2003). After being transferred onto PVDF membranes, the resolved proteins were probed with polyclonal anti-CTF. Immunoblots were detected using ECL detection reagents (Santa Cruz, CA, USA).

Anti-APP antibodies raised against the A β region of APP were obtained from Zymed (51-2700; San Francisco, CA, USA) and Sigma (A8717; St. Louis, MO, USA). Anti-phospho-JNK (9251S), anti-phospho-c-Jun (9261S), and anti-phospho-p38 (9211S) were

obtained from Cell Signaling (Beverly, MA, USA); anti-JNK3 (06-749), anti-CREB (06-504), anti-phospho-CREB (06-519), and anti-MAP2 (05-346) were obtained from Upstate Biotechnology (Lake placid, NY, USA); anti-NeuN (MAB377) and anti-calretinin (AB5054) were obtained from Chemicon (Temecula, CA, USA); anti-JNK1 (15701A) was obtained from Pharmingen (San Diego, CA, USA); anti-calbindin (C9848) and anti-parvalbumin (P3088) were obtained from Sigma (St. Louis, MO, USA); anti-JNK2 (sc-572), anti-phospho-ERK (sc-7383), anti-ERK (sc-154), p38 (sc-535-G), anti-Bcl-2 (sc-783), anti-Bad (sc-942-G), anti-Bax (sc-6236), and anti-Bcl-x_L (sc-7195) were obtained from Santa Cruz Bio-Technology (Santa Cruz, CA, USA).

For the immunohistochemistry experiments, the mice were perfused with 4% paraformaldehyde in 0.1 M phosphate buffer (PB, pH 7.4). The brain was removed and post-fixed in the same fixative at 4°C overnight. Brains were coronally cut into 40- μ m-thick sections with a vibratome. Free-floating sections were blocked by 5% normal goat serum, 2% BSA, and 2% FBS. Biotinylated HRP complex (Vector Laboratories, Burlingame, CA) and 3,3'-diaminobenzidine were used for the color development. To evaluate the neuronal loss, cresyl violet staining and anti-NeuN were performed as previously described (Che et al., 2001). Brain sections were stained with 0.5% cresyl violet. Cell counts were performed in a blind manner without knowing genotypes. To determine the cell density of cresyl violet- or anti-NeuN-stained cells in the cerebral cortex, we obtained optically dissected overlapping images covering the whole target areas (Fig. 7A) using a Polaroid DMC2 Digital Microscope Camera (Polaroid Co., Waltham, MA, USA) and computer-assisted image analysis (OPTIMAS 5.1, Bioscan Inc., USA). We found that 6 and 7 optical images were able to cover the whole target areas, respectively, in the prefrontal and parietal cortices. For cresyl-violet-stained brain sections (16–18 months), we examined total 71 sections, and, accordingly, over 460 optical images were generated and examined (Table 1).

Cell culture, transfection, and immunocytochemistry

Neuro2A cells were cultured in Dulbecco's modified Eagle's medium plus 10% fetal bovine serum (GIBCO, Grand Island, NY, USA) at 37°C in an atmosphere of 95% air and 5% CO₂. For transfection, cells were transfected with 0.2 μ g of the transgenic cassette, PDGF- β -intron- β CTF99(V717F)-pA, and 2 μ l of Oligofectamine reagent (GIBCO)/4 \times 10⁴ cells into 24-well plate. After 5 h of incubation, medium was added to Dulbecco's modified Eagle's medium containing the appropriate concentration of serum. Cells were incubated in complete medium for a period of 48 h.

After 48 h of transfection, cultured cells were fixed with 4% paraformaldehyde in 0.1 M phosphate buffer (pH 7.4) and followed by permeabilization with 0.3% Triton X-100 in phosphate-buffered saline (PBS, pH 7.4). Plates were then incubated with 5% goat serum in PBS for 1 h and incubated at 4°C overnight with 6E10 (Signet, Dedham, MA, USA) or anti-CTF [Sigma (A8717); St. Louis, MO, USA] diluted in 3% BSA. The plates were then washed with PBS and incubated with FITC- or TRITC-conjugated anti-mouse or rabbit antibody (Sigma, St. Louis, MO, USA) diluted in PBS (1:100). After washing, they were immediately mounted with fluorescent mounting medium (DAKO, Denmark) and examined under a Nikon Eclipse microscope (Nikon, Japan) or Confocal Laser Scanning Microscopy (Carl Zeiss, Jena, Germany).

Assessment of A β levels

A β levels were measured as previously described (Lee et al., 1999). Cortical tissue was homogenized in Tris-buffered saline (20 mM Tris, 137 mM NaCl, pH 7.6). The suspension was then centrifuged at $100,000 \times g$, and the supernatant containing soluble A β was collected for assay. Pellets so obtained were dissolved in 70% formic acid at a weight:volume ratio of 100 mg/ml and recentrifuged at $100,000 \times g$ for 1 h. The formic-acid-dissolved insoluble A β was collected, neutralized with 1 M Tris–Cl buffer (pH 11), and assayed. The levels of A β (1–40) and A β (1–42) peptides were analyzed using Signal Select™ Human β Amyloid A β (1–40) and A β (1–42) colorimetric sandwich ELISA kits (Signal Select™, BioSource, Camarillo, CA, USA) by following the manufacturer's instructions.

Animals and behavioral assessments

Mice were housed in clear plastic cages in a temperature- and humidity-controlled environment with a 12-h light/dark cycle (light switched on at 7 a.m.) and were maintained on an ad libitum diet of laboratory chow and water. All animals were handled in accordance with the animal care guideline of Ewha Womans University School of Medicine. To track the animals' behavior, a computerized video-tracking system called SMART (Panlab S. I., Barcelona, Spain) was used.

Open field test

Locomotor activity was measured in the open field of a white Plexiglas chamber ($45 \times 45 \times 40$ cm each). The mice were all placed in the same environment as that of the chamber 30 min prior to the test. Each mouse was placed individually in the middle of the open field, and locomotion was recorded for 60 min. The horizontal locomotor activity was judged according to the distance the animal moved. The inner 30% of the open field was defined as the center of the chamber in the current study. Illumination in the chamber was adjusted to 70 lx.

Water maze test

The water maze consisted of a 90-cm-diameter cylinder pool filled with opaque milky water (22°C). A 10-cm-diameter hidden platform was placed in a quadrant 1.5 cm below the surface of the opaque water. The pool was placed in a room with abundant environmental and artificial cues including a window, a chair, and posters. In the course of daily testing, mice were admitted successively into each of the quadrants and allowed to swim for a maximum of 90 s. On locating the platform, the animals were permitted to remain on it for 30 s before the session was terminated. The animals were tested twice a day with 6-h-intertrial interval. The latency and distance to find the platform for each of two trials and the average of the two trials were recorded for each mouse. A spatial probe trial was conducted on day 6 after the 5-day training session, which consisted of a swim trial in the absence of the hidden platform. Animals were given a single 60-s probe trial to examine memory retention.

Passive avoidance test

The test apparatus consisted of a brightly lit and a dark compartment ($15 \times 15 \times 15$ cm each), each equipped with a shock-grid floor, and a door between the two chambers. During the first day of testing, each mouse was placed in the lighted chamber

and left to habituate to the apparatus for 5 min, while allowing it to explore the light and dark rooms. On the second day, the mice were placed in the lighted chamber. After 30 s, the middle door was opened, and the latency for the mouse to enter the dark chamber was measured, which was recorded as pre-test. When the mouse entered the dark room, the door was closed, and two successive electric foot-shocks (100 V, 0.3 mA, 2 s) were delivered through the grid floor. After training, mice were then returned to their home cages. Twenty-four hours later, the mice were individually replaced in the lighted chamber, and the latency to enter the dark chamber was measured, which was recorded as post-test.

Elevated plus maze test

The elevated plus maze (EPM) apparatus consisted of four arms (30×7 cm each) made of black Plexiglas, which was elevated 50 cm above the floor and placed at right angles to each other. Two of the arms had 20-cm-high walls (enclosed arms), while the other two had no walls (open arms). The illumination at the center was adjusted to 40 lx. For the test, the mouse was initially placed at the center of the platform and left to explore the arms for 5 min. The number of entries in the open and in the enclosed arms and the time spent in each arm were recorded. Entry into each arm was scored as an event if the animal placed all paws into the corresponding arm. Methodological and conceptual issues in the use of EPM as an ethological model of provoked anxiety have been described (Rodgers and Dalvi, 1997; Wall and Messier, 2001).

Statistical analysis

Two-sample comparisons were carried out using the Student's *t* test, while multiple comparisons were made using one-way ANOVA followed by the Newman–Keuls multiple range test. All data were presented as the means \pm SEM, and statistical differences were accepted at the 5% level unless otherwise indicated.

Results

Generation of transgenic mice expressing β CTF99 in the brain

To examine the role of β CTF99 in the pathophysiology of the aging brain, we created transgenic mouse lines that carried either the PDGF- β CTF99-pA or the PDGF-intron- β CTF99-pA cassette. Both cassettes were designed to possess the APP signal sequence (17 amino acids), the A β containing C-terminal 99 amino acids of APP with the V717F mutation (β CTF99(V717F)), and the SV40 polyadenylation sequence (247 bp). Transgene expression was driven by the platelet-derived growth factor (PDGF)- β promoter, which has been used to produce a high level of transgene expression in the brain (Sasahara et al., 1991; Games et al., 1995; Irizarry et al., 1997; Lee et al., 2004). The heterologous intron (918 bp) obtained from the human β -globin gene was inserted between the PDGF- β promoter and β CTF99 in the PDGF-intron- β CTF99-pA cassette (Fig. 1A). It was found that this intron sequence greatly improved the stability of the transgene transcript (Lee et al., 2004).

We chose the inbred C57BL/6 mice as the recipient strain at the pronuclear microinjection step and at subsequent backcrosses to eliminate phenotypic variations resulting from the compound genetic backgrounds encountered in most CTF- or APP-expressing AD mouse models. A total of 16 and 2 germ-line transmittable founder lines were identified to carry PDGF- β CTF99-pA or PDGF-

intron- β CTF99-pA cassettes, respectively, as determined by genomic PCR and Southern blotting (data not shown).

Expression of transgene transcript and protein products in the brain

To determine transgene expression, total RNA was prepared from the brains of F1 progeny at 2 months of age. In Northern blots, the 32 P-labeled C-terminal *SpeI* fragment hybridized with two bands: the upper ~ 3.5 kb fragment of the endogenous mouse APP transcript and the lower ~ 700 bp transcript derived from the transgene (Fig. 1B). Based on RT-PCR and Northern blot analyses, we chose the β CTF99-#F17 line which showed highest transgene expression in the brain and renamed this Tg- β CTF99/B6. By Northern blotting, it was estimated that the relative amount of transgene expression in the heterozygous state was higher than the expression of the endogenous APP transcript (Fig. 1B).

Western blots using two β CTF-specific polyclonal antibodies commonly detected the endogenous ~ 12 kDa β CTF99 and ~ 10 kDa α CTF83 (p3) fragments, which were generated by β - and α -secretases, respectively, in the brains of non-transgenic controls (Fig. 2A). In the Tg- β CTF99/B6 brain at 4–5 months, the amounts of β CTF99 and α CTF83 were notably up-regulated. Densitometric measurements of the CTFs using computer-assisted imaging software indicated that the expression levels of β CTF99 and α CTF83 were 2.26 ± 0.19 and 2.36 ± 0.11 -fold that of endogenous β CTF99 and α CTF83. Consistent with these results, immunohistological staining revealed β CTF99 up-regulation in neuronal cells in broad regions of the brain, including the prefrontal cortex (Figs. 2B–E). However, senile plaque-like A β -deposition or Congo-Red-positive amyloid was not detected in Tg- β CTF99/B6 mice up to 18 months of age. Moreover, extensive gliosis that can be ascribed to a marker of plaque formation or cell death was absent in the cerebral cortices and hippocampal regions of Tg- β CTF99/B6 at 14–16 months. Approximately 92% of the Tg- β CTF99/B6 mice survived until at least 480 days (16 months) versus 100% of the non-transgenic controls.

The endogenous CTF is known to be concentrated in ER and Golgi compartments (Xia et al., 1998). To confirm that the subcellular distribution of β CTF99 that is transcribed from the transgenic cassette, PDGF- β -intron- β CTF99(V717F)-pA, mimics the subcellular distribution of endogenous CTF, we performed an in vitro transfection experiment in neuro2A cells. Forty-eight hours after transfection of the transgenic cassette, transfected cells and controls were stained with 6E10, which is specific to the A β region of human APP and with a CTF-specific antibody, which specifically reacts with the A β region of human and mouse CTF(s). The resulting data indicated that the transfected CTF99 was distributed asymmetrically in the cytoplasm and in the proximal neuritic processes of neuro2A cells (Figs. 2F–H). This asymmetrical subcellular localization pattern resembled transgenic β CTF99 expression in the cortical neurons of Tg- β CTF99/B6 mice (Figs. 2D and E).

Expression of cell-death-related proteins in the Tg- β CTF99/B6 brain

We investigated whether the transgenic expression of β CTF99 produced biochemical changes characteristic of the human AD brain. Recent reports indicating that the human AD

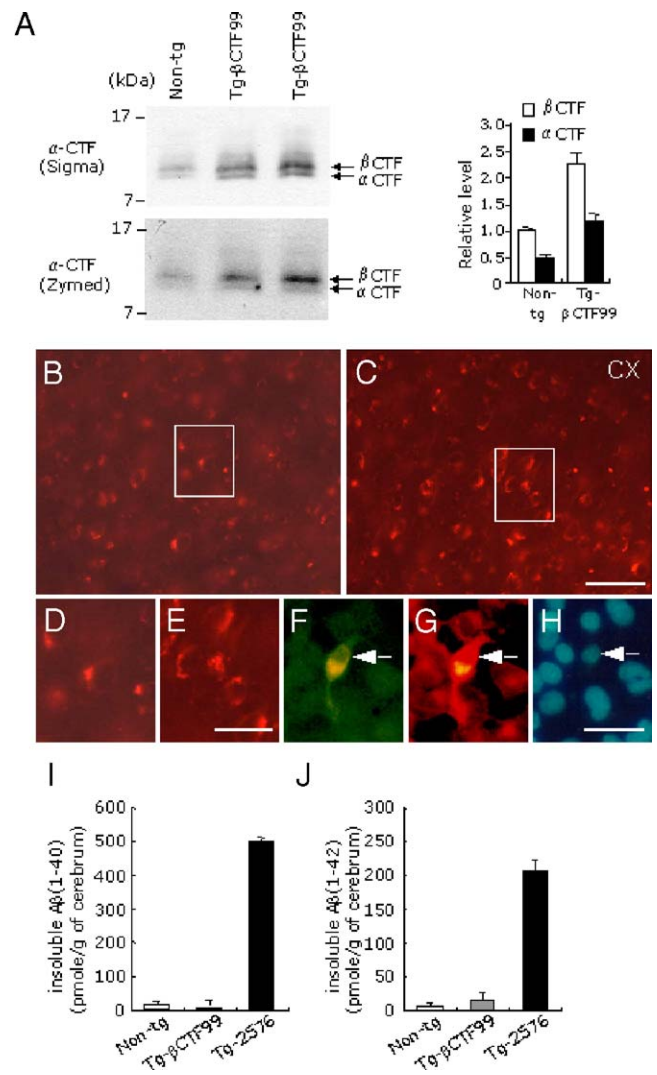


Fig. 2. Western blot and immunological analyses of the transgenic expression of β CTF99. (A) Anti-C-terminal fragment of APP antibody from Sigma (A8717) detected the increased β CTF99 and α CTF83 production in the Tg- β CTF99/B6 brain (left panel, top). Anti-CTF of APP from Zymed showed a similar expression pattern (left panel, bottom). The levels of β CTF99 and α CTF83 in the heterozygous state were quantified with respect to the β CTF99 expression level of the non-transgenic control (right panel). Data presented are the means \pm SEM of 4 independent experiments on 5 animals. non-Tg, non-transgenic control; β CTF99, Tg- β CTF99/B6. (B, C) Immunohistochemical detection of transgenic β CTF99 with the anti-CTF of APP (Sigma; A8717) in the prefrontal cortex (CX) of Tg- β CTF99/B6 at 15 months (C) and in the non-transgenic control (B). Scale bar: 100 μ m. (D, E) High magnification images of the areas marked with squares in panels B and C. Scale bars: D and E, 50 μ m. (F–H) Immunocytochemical staining of neuro2A cells transfected with the transgenic cassette PDGF- β -intron- β CTF99(V717F)-pA, which was used to generate the Tg- β CTF99/B6 mouse line, as described in Materials and Methods. Transfected cells (marked with an arrow) were stained with 6E10 (FITC labeled; F), which is specific for the A β region of human APP, and with anti-CTF of APP (Sigma; A8717) (TRITC labeled; G), which reacts with the A β region of human and mouse CTF. Stained cells were also incubated with Hoechst 33342 to visualize the nuclei (H). Scale bars: F–H, 50 μ m. (I, J) A β (1–40) and A β (1–42) levels in the brain of 15-month-old Tg- β CTF99/B6 mice were measured using ELISA assays. A β (1–40) and A β (1–42) levels in Tg2576 (Hsiao et al., 1996) at 13 months were used as controls. The data are shown as means \pm SEM (3 Tg- β CTF99/B6, 3 non-transgenic controls, and 2 Tg2576 mice were used).

brain shows phospho-JNK up-regulation (Zhu et al., 2001; Savage et al., 2002) prompted us to examine the levels of phospho-JNK, -ERK, -p38 MAPKs, and phospho-c-Jun in the Tg- β CTF99/B6 brain. It was found that the levels of phospho-JNK and phospho-c-Jun in the whole cerebrum homogenate of Tg- β CTF99/B6 at 15 months were notably higher than those of age-matched controls, whereas the expressions of JNK1, JNK2, JNK3, phospho-ERK, and phospho-p38 were not significantly changed (Fig. 3).

Next, we examined whether the transgenic expression of β CTF99 affected the expressions of the B-cell leukemia-2 (Bcl-2) family proteins, of which Bcl-2 and Bcl-x_L are anti-apoptotic whereas Bad and Bax are pro-apoptotic (Davies, 1995). Western blot analysis indicated that the expressions of Bcl-2 and Bax were significantly elevated, whereas Bcl-x_L expression was attenuated in whole cerebrum homogenate of Tg- β CTF99/B6 mice at 14–16 months (Fig. 4A). Immunostaining showed the increased Bad and Bax expression in the pyramidal cell layer of the hippocampus (Figs. 4B–E).

Expression of calcium-binding protein in the Tg- β CTF99/B6 brain

The human AD brains showed the reduced expression of calcium-binding proteins (Iacopino and Christakos, 1990; Mikko-

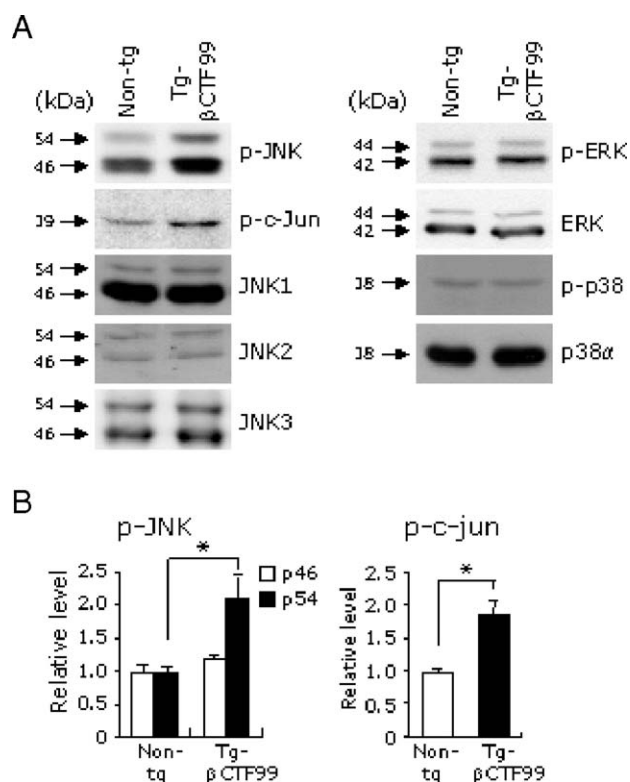


Fig. 3. Activation of the JNK pathway in the Tg- β CTF99/B6 brain. (A) Western blots showed elevated phospho-JNK (P-JNK) and phospho-c-Jun (P-c-Jun) expression in the whole cerebrum homogenate of Tg- β CTF99/B6 at 15 months. The expressions of JNK1, JNK2, JNK3, phospho-ERK (p-ERK), and phospho-p38 (P-p38) were unchanged. (B) Expression levels of phospho-JNK (left panel) and phospho-c-Jun (right panel) were quantified. Data presented are the means \pm SEM of 7 and 4 independent experiments on 6 and 4 animals for p-JNK and phospho-c-Jun, respectively. * Indicates a difference at the $P < 0.05$ level in each group.

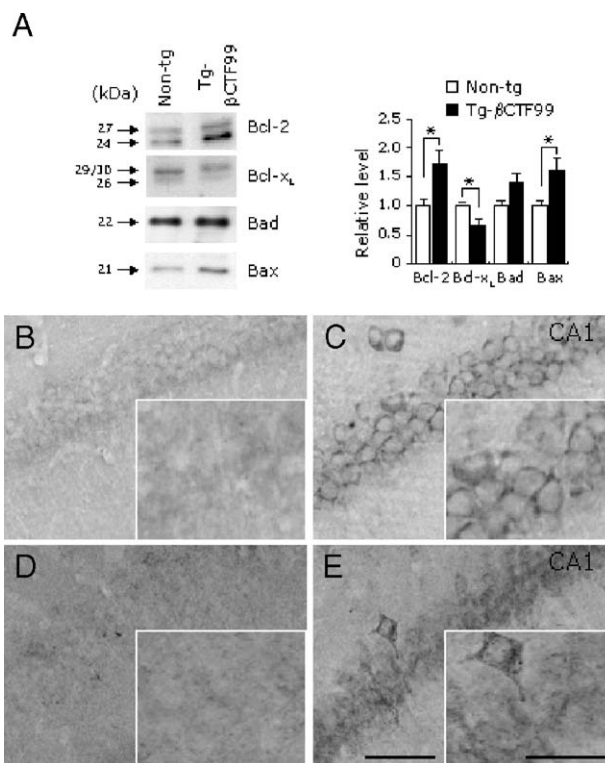


Fig. 4. Altered expression of Bcl-2 family proteins in the Tg- β CTF99/B6 brain. (A) Western blots showing the expressions of Bcl-2, Bad, Bax, and Bcl-x_L in whole cerebrum homogenate of Tg- β CTF99/B6 at 14–15 months and their control. The expression levels of Bcl-2 family proteins were quantified (right panel). Data presented are the means \pm SEM of 7 independent experiments on 5 animals. (B–E) Immunohistological staining showing increased Bad (B, C) and Bax (D, E) expression in the pyramidal layer of CA1 of Tg- β CTF99/B6 at 15 months (C and E) and in age-matched non-transgenic controls (B and D). Insets in panels B–E are high magnification images of CA1 pyramidal cells. Scale bars: B–E, 50 μ m; insets in B–E; 25 μ m. * Indicates a difference at the $P < 0.05$ level in each group.

nen et al., 1999). In the present study, Western blotting indicated that calbindin (CB) expression was significantly reduced in the whole cerebrum homogenate of Tg- β CTF99/B6 at 14–16 months versus the non-transgenic control (Fig. 5A). In agreement with these results, CB immunoreactivity was notably reduced in the neocortex, and in CA1 and CA3, and in the dentate gyrus of Tg- β CTF99/B6 versus the non-transgenic controls (Figs. 5F–K). Moreover, this diminished CB expression was detectable in the brains of Tg- β CTF99/B6 mice at 12 months, but not at 5 months (Figs. 5B–E). Immunohistochemical and Western blot analyses indicated that the expression levels of the other two calcium binding proteins, parvalbumin and calretinin, in the hippocampal regions were similar for Tg- β CTF99/B6 and age-matched controls (data not shown).

Impaired phosphorylation of CREB in the Tg- β CTF99/B6 brain

Phosphorylated CREB (phospho-CREB) levels are reduced in the AD brain (Yamamoto-Sasaki et al., 1999). Western blot analysis in the current study indicated that the level of phospho-CREB in the whole cerebrum homogenate of Tg- β CTF99/B6 at 14–16 months was lower than that of the non-transgenic control

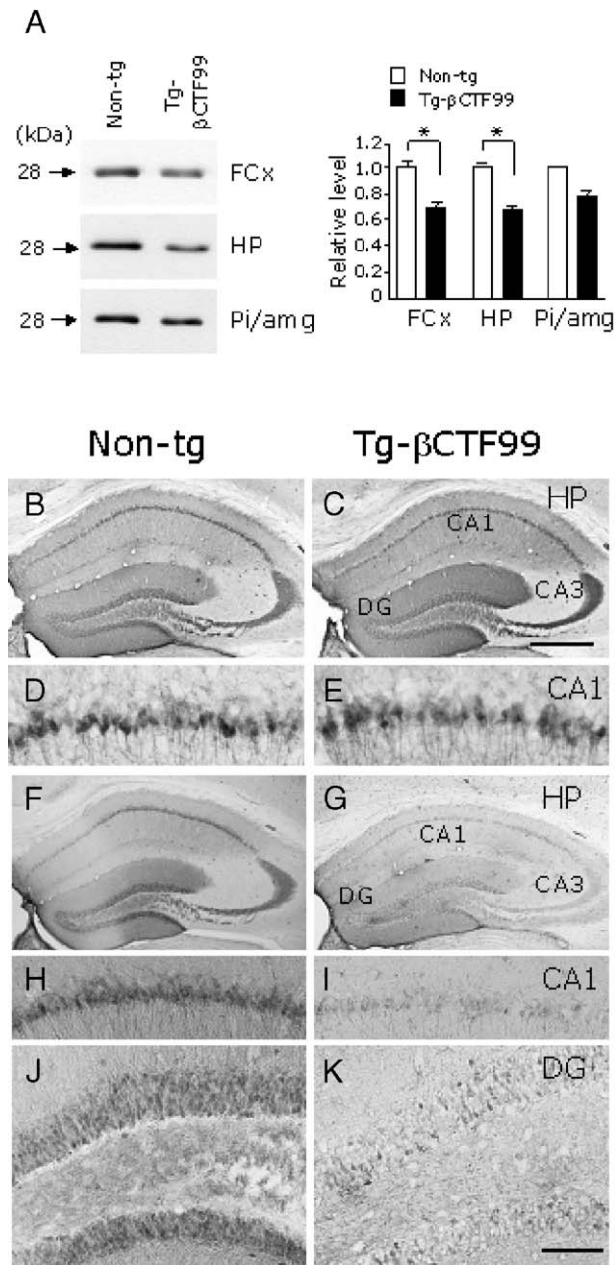


Fig. 5. Reduced expression of calbindin in the Tg-βCTF99/B6 brain. (A) Representative Western blots showing calbindin expression in the prefrontal cortex (FCx), hippocampus (HP), and piriform cortex/amygdala (Pi/amg) of Tg-βCTF99/B6 at 15 months (left panel). Calbindin expression was quantified (right panel). The data are the means ± SEM of 6 independent experiments on 5 animals. (B–K) Immunohistological staining showing calbindin expression in CA1 pyramidal cells (D, E, H, and I) and in granule cells of the dentate gyrus (J and K) of Tg-βCTF99/B6 at 5 months (C and E) or at 15 months (G, I, and K) and of age-matched non-transgenic controls at 5 months (B and D) or 15 months (F, H, and J). HP, hippocampus; DG, dentate gyrus. Scale bars: C, 500 μm; K, 100 μm. * Indicates a difference at the $P < 0.05$ level in each group.

(Fig. 6A). Immunohistological staining indicated that phospho-CREB expressions in the neocortex and in the pyramidal layer of the hippocampus were reduced in Tg-βCTF99/B6 at 14–16 months (Figs. 6F–M), and similarly reduced phospho-CREB expression was also detected in Tg-βCTF99/B6 at 12 months

(data not shown). However, the level of phospho-CREB in Tg-βCTF99/B6 at 5 months was similar to that of the non-transgenic control (Figs. 6B–E). In addition, c-Fos immunoreactivity was significantly repressed in the neocortex and in the hippocampal regions of Tg-βCTF99/B6 at 12 months versus the non-transgenic controls (Figs. 6N and O).

Progressive neuronal loss in the aged Tg-βCTF99/B6 brain

To examine the possibility of age-dependent neuronal loss in the Tg-βCTF99/B6 brain, we measured cell densities in the prefrontal and parietal cortices after staining coronal sections of the non-transgenic control and Tg-βCTF99/B6 brains with cresyl violet. The areas counted in the prefrontal cortex spanned the following areas: from dorsal to ventral, the cingulate cortex, the primary and secondary motor cortices, and the primary and secondary sensory cortices, and in the parietal cortex, again from dorsal to ventral, the retrosplenial cortex, the primary sensory cortex, the posterior parietal association area, and the auditory cortex (Franklin and Paxinos, 1997; Fig. 7A). The thicknesses of the primary sensory cortex in the prefrontal cortex and the posterior parietal association area in the parietal cortex of Tg-βCTF99/B6 at 16–18 months versus the non-transgenic control were, respectively, 1.268 ± 0.018 mm versus 1.264 ± 0.026 mm ($P > 0.05$, Student's t test) and 0.691 ± 0.02 mm versus 0.688 ± 0.02 mm ($P > 0.05$, Student's t test). The thicknesses of the prefrontal and parietal cortices in other counted regions were also comparable in both groups of mice.

We determined the cell density of anti-NeuN-stained cells in the prefrontal or parietal cortex after preparation of overlapping optical images covering the target areas, as described in Materials and methods. We counted anti-NeuN-stained or cresyl-violet-stained cells in each optical image without knowing genotypes. The cell density of anti-NeuN-stained cells in the prefrontal cortex of the 16- to 18-month Tg-βCTF99/B6 brain was determined to be $85.1 \pm 4.2\%$ of the age-matched non-transgenic control ($2572 \pm 233/\text{mm}^2$ in Tg-βCTF99/B6 versus $3023 \pm 58/\text{mm}^2$ in the non-transgenic control; $P < 0.05$, Student's t test) (Figs. 7B and C). Similarly, the cell density of anti-NeuN-stained cells in the parietal cortex of the 16- to 18-month Tg-βCTF99/B6 brain was $87.5 \pm 3.6\%$ of the age-matched non-transgenic control ($3147 \pm 47/\text{mm}^2$ in Tg-βCTF99/B6 versus $3597 \pm 140/\text{mm}^2$ in the non-transgenic control; $P < 0.05$, Student's t test). The thickness of anti-NeuN-stained pyramidal layer of the hippocampal CA1 region of Tg-βCTF99/B6 was reduced compared to that of the non-transgenic control (Figs. 7D and E). Consistent with these results, anti-MAP2 staining showed severe atrophy of large apical dendrites of pyramidal neurons in various cortical regions including the prefrontal and parietal cortices of Tg-βCTF99/B6 at 16–18 months (Figs. 7F and G).

We counted cresyl-violet-stained cells in the prefrontal or parietal cortex, as was for anti-NeuN-stained brain sections. The resulting data were summarized in Table 1. The cresyl violet was found to stain not only neurons, but also some glia, and most stained neurons are distinguishable from glia because of their distinct cell morphology and staining intensity. The cell density of cresyl-violet-stained cells in the prefrontal cortices of the 16- to 18-month Tg-βCTF99/B6 brain was determined to be $85.3 \pm 1.34\%$ of the age-matched non-transgenic control ($3227 \pm 139/\text{mm}^2$ in Tg-βCTF99/B6 versus $3785 \pm 101/\text{mm}^2$ in the non-

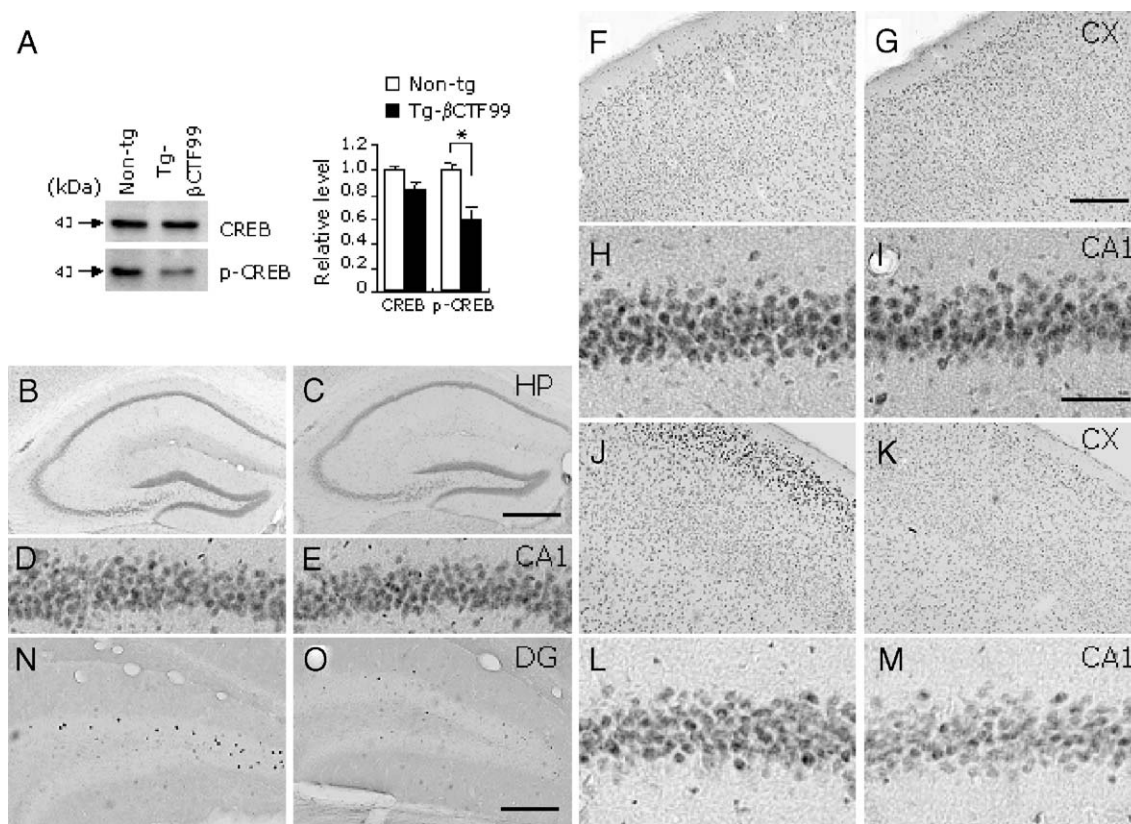


Fig. 6. Reduced expression of phospho-CREB and c-Fos in the Tg-βCTF99/B6 brain. (A) Representative Western blots showing CREB and phospho-CREB expression in the hippocampus of Tg-βCTF99/B6 at 15 months. Expression levels of CREB and phospho-CREB were quantified (right panel). Data are the means \pm SEM of 5 independent experiments on 4 animals. (B–M) Immunohistological staining for phospho-CREB (B–E, J–M) and CREB (F–I) expression in the prefrontal cortex (F, G, J, and K) and in CA1 pyramidal cells (D, E, H, I, L, and M) of Tg-βCTF99/B6 (C, E, G, I, K, and M) and non-transgenic controls (B, D, F, H, J, and L). (N and O) Reduced expression of c-Fos in the dentate gyrus of Tg-βCTF99/B6 at 12 months (O) and in age-matched control (N). HP, hippocampus; CX, prefrontal cortex; DG, dentate gyrus. Scale bars: C, 500 μ m; I, 50 μ m; G and O, 200 μ m. * Indicates a difference at the $P < 0.05$ level in each group.

transgenic control; $P < 0.05$, Student's t test). Similarly, the cell density of cresyl-violet-stained cells in the parietal cortex of Tg-βCTF99/B6 at 16–18 months was reduced to $89.7 \pm 0.65\%$ of that of the non-transgenic control ($3752 \pm 92/\text{mm}^2$ in Tg-βCTF99/B6 versus $4185 \pm 134/\text{mm}^2$ in the non-transgenic control; $P < 0.05$, Student's t test) (Table 1; Figs. 7I–K). At 5 months, however, cresyl-violet-stained cell densities in the prefrontal cortices of Tg-βCTF99/B6 versus non-transgenic controls were, respectively, $4989 \pm 99/\text{mm}^2$ versus $4889 \pm 154/\text{mm}^2$ and in the parietal cortices $5558 \pm 61/\text{mm}^2$ versus $5567 \pm$

$188/\text{mm}^2$, respectively ($P > 0.05$ in both cases; Student's t test) (Fig. 7H). Anti-MAP2-stained dendritic morphologies of pyramidal neurons between Tg-βCTF99/B6 at 5 months and their control mice were indistinguishable (data not shown).

Tg-βCTF99/B6 at 11–14 months showed normal locomotor activity

The altered expressions of biochemical markers and the histological deterioration observed in the Tg-βCTF99/B6 brain

Table 1

The parameters and values for cresyl-violet-stained cell densities in the prefrontal and parietal cortices of Tg-βCTF99/B6 at 16–18 months and of their non-transgenic controls

	Prefrontal cortex		Parietal cortex	
	Non-Tg control	Tg-βCTF99/B6	Non-tg control	Tg-βCTF99/B6
Animals examined (total brain sections counted)	7 (16)	8 (17)	6 (18)	7 (20)
Counted area	6.10 ± 0.09 (mm^2)	6.44 ± 0.1 (mm^2)	4.73 ± 0.05 (mm^2)	4.42 ± 0.05 (mm^2)
Thickness ^a	1.264 ± 0.03 (mm)	1.268 ± 0.02 (mm)	0.688 ± 0.02 (mm)	0.691 ± 0.02 (mm)
Cell numbers ^a	23530 ± 675.6	20838 ± 917.8	19848 ± 691.7	16564 ± 461.9
Cell density ^b	3785.6 ± 101.5 (mm^2)	3227.4 ± 139.4 (mm^2)	4185.1 ± 133.9 (mm^2)	3752.3 ± 92.3 (mm^2)
P value (Student's t test)	$P = 0.003$ ($P < 0.01$)		$P = 0.01$ ($P < 0.05$)	

^a The thickness was measured at the primary sensory cortex in the prefrontal cortex and at the posterior parietal association area in the parietal cortex.

^b Cell numbers and cell density in the respective region were determined for each brain section, and averaged values (means \pm SEM) are shown.

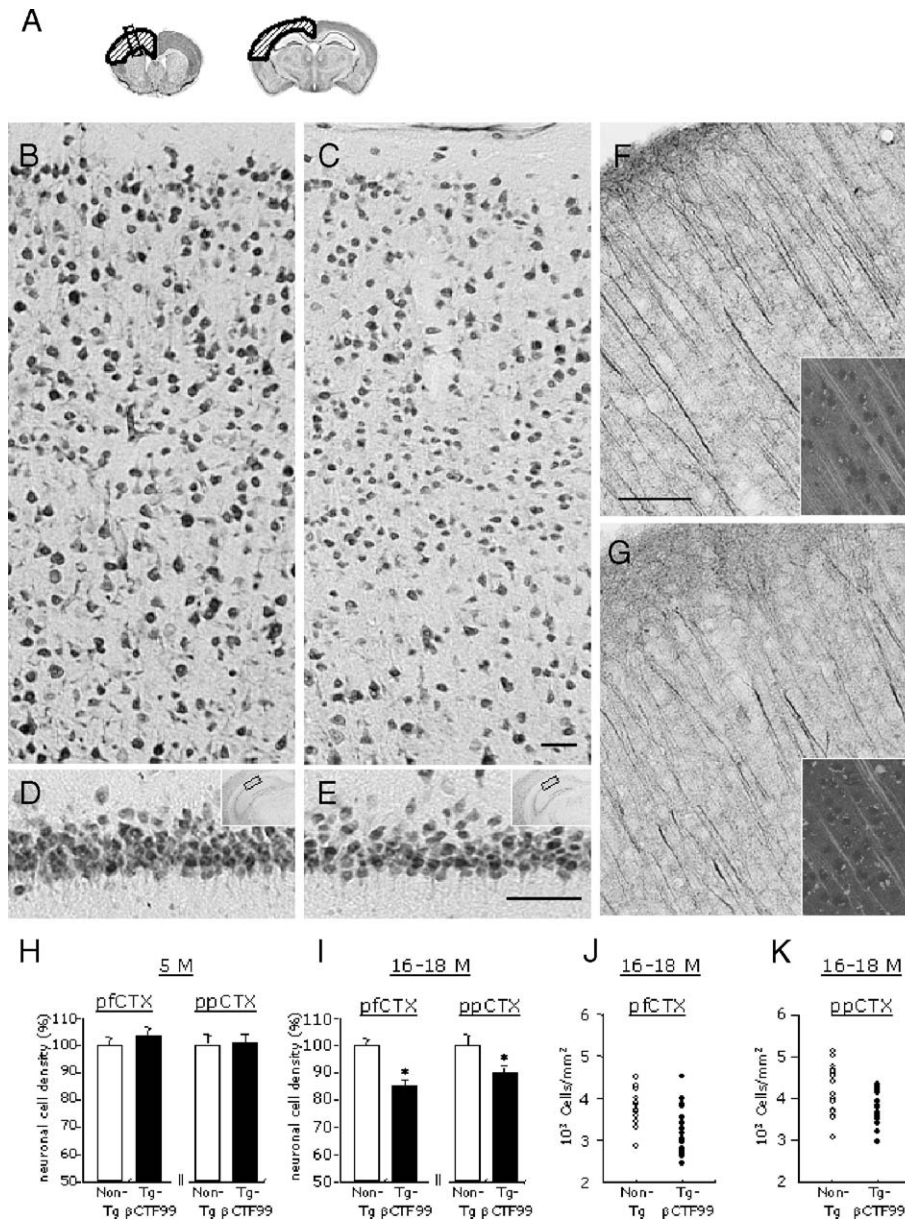


Fig. 7. Reduced cell density and dendritic atrophy of pyramidal neurons in the parietal cortices of 18-month-old Tg-βCTF99/B6 mice. (A) Cortical areas counted in the prefrontal (left panel) and parietal (right panel) cortices are indicated (hatched areas). Counted areas represent approximately 66.4–67.9% for the prefrontal cortex and 41.1–43.3% for the parietal cortex of the total cerebral cortex of a hemisphere in each coronal section of the brain. For each cortical area, 2–4 brain sections on 7–8 Tg-βCTF99/B6 mice at 16–18 months and 6–7 non-transgenic controls were examined. (B–E) Representative photomicrographs showing the anti-NeuN-stained prefrontal cortices (B, C) and anti-NeuN-stained pyramidal cells (D, E) of the hippocampal CA1 regions (insets) of Tg-βCTF99/B6 at 18 months (C, E) and their non-transgenic controls (B, D). The photographed images (B, C) are from the prefrontal cortex indicated by a rectangle in the left panel of A. (F, G) Posterior parietal cortices stained with peroxidase/DAB-labeled anti-MAP2 or Texas-Red-labeled anti-MAP2 (insets) are presented. Presented peroxidase/DAB-labeled and Texas-Red-labeled images are from independent individuals at 18 months. (H–K) The cell densities (H, I) of cresyl-violet-positive cells in the prefrontal (pfCTX) and posterior parietal (ppCTX) cortices of Tg-βCTF99/B6 mice at 5 (H) or 16–18 (I–K) months and their non-transgenic controls, and scatter plots of data points (J, K) are shown. Scale bars: C and G, 100 μm. E, 50 μm.

prompted us to investigate their behavioral and psychological responses. With respect to the spontaneous motor activities, such as walking, running, climbing, grasping, writhing, and motor skills related to eating, Tg-βCTF99/B6 mice at up to 20 months were indistinguishable from the corresponding non-transgenic animals. In an open field test, the locomotor activities displayed by Tg-βCTF99/B6 mice at 11 months or 14 months were similar to those of age-matched controls (data not shown).

Impaired cognitive function of Tg-βCTF99/B6

To assess the cognitive function of Tg-βCTF99/B6 mice, we used the Morris water maze test and the passive avoidance test. Mice were trained to perform a hidden platform task in the Morris water maze. The performance of non-transgenic control mice at 7, 12.5, and 14.5 months old progressively improved after trials. Whereas the times required for Tg-βCTF99/B6 to find the hidden platform gradually increased versus the age-matched non-trans-

genic controls, the escape latency of Tg-βCTF99/B6 at 12.5 and 14.5 months remained to be higher than that of the control animals ($P < 0.05$, $n = 8-15$) (Figs. 8A–B). In a probe trial test, Tg-βCTF99/B6 mice at 12.5 months showed reduced dwelling time in the target quadrant compared to that of the control animals (Fig. 8C). In the visual platform version of the Morris water maze, Tg-βCTF99/B6 at 12.5 months showed a good performance as much as the age-matched controls did (Fig. 8D).

In the passive avoidance test, the latency to enter the dark chamber was similar for Tg-βCTF99/B6 and control at 7 months. However, the post-shock latency for the Tg-βCTF99/B6 mice was shorter than that of the non-transgenic controls (Fig. 8E). This impaired memory retention of Tg-βCTF99/B6 mice was also clearly observable at 10 months (data not shown) and at 14 months (Fig. 8E).

The increased anxiety shown by Tg-βCTF99/B6 mice

Increased anxiety is a problematic symptom of human AD (Chemerinski et al., 1998; Folstein and Bylsma, 1999; Chung and Cummings, 2000; Ownby et al., 2000). Histological deterioration and various biochemical alterations in the brain led us to examine the anxiety-related behaviors of Tg-βCTF99/B6 mice. In the elevated plus maze, the number of entries and the time spent in the open arm for Tg-βCTF99/B6 mice at 5 months were indistinguishable from those of the non-transgenic controls (data not shown). In contrast, Tg-βCTF99/B6 mice at 11 months visited the open arm less frequently and spent less time there than age-

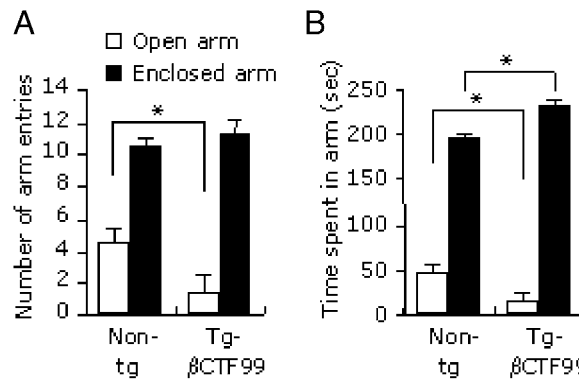


Fig. 9. Increased anxiety shown by Tg-βCTF99/B6. (A, B) Tg-βCTF99/B6 at 13 months showed a lower number of entries and spent less time in the open arm of the elevated plus maze than age-matched non-transgenic controls. Means ± SEM are shown (10 controls and 7 Tg-βCTF99/B6 mice were used). * Indicates a difference at the $P < 0.05$ level in each group.

matched non-transgenic controls (Fig. 9), which suggest that the Tg-βCTF99/B6 mice showed increasing anxiety with age.

Discussion

The current study was undertaken to examine the role of the Aβ-bearing carboxy-terminal fragment of APP, βCTF99, in the pathophysiology of the aging brain, using a novel transgenic

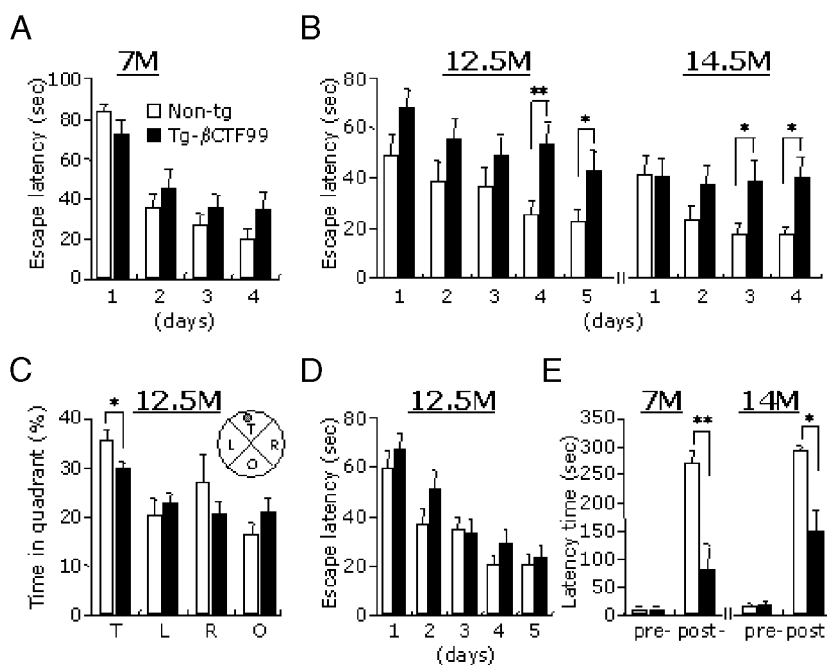


Fig. 8. Altered cognitive functions of Tg-βCTF99/B6 mice. (A, B) Escape latencies of Tg-βCTF99/B6 at 7 (A), 12.5, or 14.5 (B) months and of their age-matched controls in the hidden platform version of the Morris water maze. Naive mice of 8 controls and 7 Tg-βCTF99/B6 were examined at 7 months. Naive mice of 7 controls and 8 Tg-βCTF99/B6 were examined at 12.5 months and reexamined at 14.5 months. (C) A spatial probe trial test. Following the 5-day training session as shown in panel B, Tg-βCTF99/B6 mice at 12.5 months and their control mice were placed in a spatial probe trial test. The percentage of time spent in the target quadrant was determined (means ± SEM) during probe trials. The dashed line represents chance performance levels (25%). Filled column: Tg-βCTF99/B6. Open column: non-transgenic littermates (* for $P < 0.05$). (D) Escape latencies of Tg-βCTF99/B6 at 12.5 months and of their age-matched controls in the visual platform version of the Morris water maze. (E) Memory retention in the passive avoidance test for Tg-βCTF99/B6 at 7 or 14 months. Memory retention of Tg-βCTF99/B6 at 11 months was also defective (not shown). Ten controls and 10 Tg-βCTF99/B6 were used at 7 months and 14 controls and 9 Tg-βCTF99/B6 at 14 months. Pre-, pre-shock; Post-, post-shock. Means ± SEM are presented. * and ** indicate differences at the $P < 0.05$ and $P < 0.01$ levels, respectively, in each group.

mouse line, Tg- β CTF99/B6, created from the C57BL/6 inbred strain. As demonstrated by this study, the transgenic expression of β CTF99 produced progressive detrimental changes in the brains of mice, which emulated the important pathological and behavioral features of human AD.

The transgenic strategy used in generating Tg- β CTF99/B6

The major factors that made it possible to generate the transgenic Tg- β CTF99/B6 mouse line were as follows. Firstly, the transgenic cassette used in Tg- β CTF99/B6 contained the APP signal sequence (17 amino acids) immediately followed by the A β bearing C-terminal 99 amino acids of APP containing the V717F Indiana mutation. After the signal sequence has been clipped-off, β CTF99(V717F) is supposed to correctly orientate in the membrane like the endogenous β -secretase cleaved CTF of APP. Therefore, the β CTF99(V717F) expressed in Tg- β CTF99/B6 mice is expected to have the same topographical configuration as that of natural β CTFs or more precisely of the C-terminal part of APP. Our *in vitro* analysis of the expression of β CTF99 in neuro2A cells and the observed transgenic expression pattern of β CTF99 in the brain *in vivo* supported our initial intentions (Fig. 2). Secondly, the heterologous intron was inserted immediately after the PDGF β promoter, which led to Tg- β CTF99/B6 that expresses the transgene at a level 2.3-fold of that of endogenous CTF, as determined by Western blotting. We speculate that this up-regulation of β CTF99 is essentially required to produce the observed pathophysiological signs of the AD-like brain because mouse lines expressing lower levels of the same transgene did not produce the same distinctive phenotypes, even when they reached an age of 12–18 months (data not shown). Thirdly, the Tg- β CTF99/B6 mouse line was established from the C57BL/6 inbred strain. Adopting this strategy basically eliminated the possibility of phenotypic variations resulting from compound genetic backgrounds, as encountered in other CTF- or APP-expressing transgenic lines. In fact, previously created CTF-expressing transgenic lines have compound genetic backgrounds, such as the C57BL/6–DBA/2 hybrids (Li et al., 1999; Rutten et al., 2003), the C57BL/6–SJL hybrids (Kammesheidt et al., 1992; Fukuchi et al., 1996; Oster-Granite et al., 1996), or the C3H–C57BL/6 hybrids (Nalbantoglu et al., 1997; Sato et al., 1997). We speculate that these complicated genetic backgrounds and different topographic configuration of expressed CTFs with respect to the cellular membrane, and transgene expression levels, contribute to the diversity of published data on the role of CTFs in the aging brain. The genetic strategy used in our Tg- β CTF99/B6 mouse line should confer on them many additional advantages over other AD models, given that the phenotypic variation between individuals is minimized, which highly simplifies studies involving genetic intercrosses with other transgenic animals and reduces the need for multiple control lines.

We originally obtained 16 and 2 germ-line transmittable founder lines that carried the PDGF- β CTF99-pA or the PDGF-intron- β CTF99-pA cassette, respectively, although similar amounts of efforts had been put in both transgenic cases. In addition, all PDGF- β CTF99 founder lines and 1 out of 2 PDGF-intron- β CTF99-pA founder lines expressed the transgene at very low levels, and most biochemical and behavioral phenotypes of these lines were either not expressed or subtle. These results may suggest the importance of the intron in our transgenic cassettes to ensure high levels of transgene expression and also the difficulty in

obtaining mice expressing high levels of β CTF99. We admit that it might be a limitation of this study to describe phenotypes of Tg- β CTF99/B6 mice based on a transgenic line, and it remains to be more rigorously tested in the future that the potential transgene integration-induced mutation contributes to any of the observed abnormalities. Nonetheless, we are convinced that biochemical and behavioral phenotypes of Tg- β CTF99/B6 mice are due to the expression of β CTF99/B6 because of following reasons. First, all phenotypes described are expressed in an age-dependent manner or in aged brains, as in the cases of other known AD models. Second, independently generated Tg-APP/B6 mice expressing a mutant form of APP also show phenotypes similar to those of Tg- β CTF99/B6. Tg-APP/B6 mice showed enhanced β CTF99 expression originated from the APP transgene. Both Tg- β CTF99/B6 and Tg-APP/B6 mice showed reduced calbindin expression in the dentate gyrus. Reduced calbindin expression is also detected in aged Tg2576 mice, not in young Tg2576 mice (our unpublished data), and reduced calbindin expression is known to be a histological feature of the AD brain (Iacopino and Christakos, 1990; Mikkonen et al., 1999). Third, our preliminary data show that the biochemical and behavioral phenotypes of both homozygote and heterozygote of Tg- β CTF99/B6 mice are produced progressively and age-dependently, but only in aged animals, though phenotypes displayed by homozygous Tg- β CTF99/B6 are generally stronger than those of heterozygote.

Neuropathological features of Tg- β CTF99/B6 as an AD model

Tg- β CTF99/B6 mice showed a progressive and age-dependent reduction in the expression of calbindin and phospho-CREB, neuronal loss in the brain, cognitive deficits, and increased anxiety, all of which are characteristic features of the human AD brain. Each of these features probably justifies more detailed discussion.

First, Tg- β CTF99/B6 mice at 14–15 months showed severely attenuated calbindin (CB) expression in several brain regions including the hippocampus (Fig. 4). Calbindin, together with parvalbumin (PV) and calretinin (CR), constitutes the calcium-binding proteins that label GABAergic and pyramidal-shaped neurons in various areas of the brain (Iacopino and Christakos, 1990; Leuba et al., 1998; Bu et al., 2003). These calcium-binding proteins regulate intracellular calcium concentrations due to their calcium buffering capacities. Moreover, altered intracellular calcium homeostasis may impair normal cellular function, including synaptic plasticity, and/or potentiate the cytotoxicity of neural cells (Mattson et al., 1993; Mattson, 1998; Berridge, 1998; Carafoli, 2002). Mice deficient in CB were found to show impairments in spatial learning and LTP (Molinari et al., 1996). Moreover, in aging or neurodegenerative brains, CB expression was reduced, and this may be related to pathologic changes (Iacopino and Christakos, 1990; Leuba et al., 1998; Bu et al., 2003). Despite the development of numerous AD models, the correlation between CB depletion and cognitive deficits has been described only recently in transgenic lines expressing mutant forms of human APP (Palop et al., 2003; Lee et al., 2004). It would be interesting to explore the mechanisms determining how the age-dependent decline in brain CB expression of the Tg- β CTF99/B6 model leads to impaired cognition and other AD-like pathophysiology.

Second, Tg- β CTF99/B6 at 12–16 months showed phospho-CREB down-regulation in many brain regions including the hippocampus. CREB phosphorylation is known to increase during

neural activity and to lead to long-lasting synaptic plasticity, especially in hippocampus-dependent memory (Mayford and Kandel, 1999; Viola et al., 2000; Colombo et al., 2003). Moreover, antisense oligodeoxynucleotide-mediated disruption of the CREB gene in the hippocampus was found to impair long-term memory formation (Guzowski and McGaugh, 1997), and a targeted mutation of the CREB β -isoform was associated with abnormal learning and memory (Bourtchuladze et al., 1994; Blendy et al., 1996), whereas increasing the level of CREB in the brain enhanced the formation of long-term memory (Josselyn et al., 2001). In the Alzheimer's brain, phospho-CREB levels were found to be attenuated without any accompanying change in total CREB protein, in addition, the CREB-related intracellular signaling pathway was found to be disturbed (Yamamoto-Sasaki et al., 1999). These results suggest that the age-dependent cognitive impairment of Tg- β CTF99/B6 mice could be related to a CREB-related signaling pathway. Moreover, CREB activity in the nucleus accumbens was found to influence anxiety-like behavioral responses (Barrot et al., 2002). And, because Tg- β CTF99/B6 mice showed anxiety-like behaviors in the elevated plus maze (Fig. 9), the mechanism determining the role of CREB in the progressive generation of anxiety may be worthy of exploration in the future.

Third, Tg- β CTF99/B6 mice at 14–15 months showed many biochemical and histological markers of an AD pathophysiology. These mice showed some similarities with the Tg2576 + PS1P264L double transgenic mouse model of Savage et al. (2002) as both AD models showed increased JNK pathway activation, a feature displayed by the human AD brain (Zhu et al., 2001; Savage et al., 2002). These results support the known strong correlation between β CTF99 or its products and increased JNK pathway activation in the pathogenesis of AD. In addition, Tg- β CTF99/B6 mice at 14–15 months showed altered Bcl-2 family protein expressions in the brain. The expressions of Bcl-2, Bad, and Bax in brain were increased, whereas Bcl-x_L expression was reduced in Tg- β CTF99/B6 mice at 14–15 months, thus indicating unbalanced Bcl-2 family protein expressions in the brain. These altered expression patterns of the Bcl-2 family proteins in the brain of Tg- β CTF99/B6 mice resemble the increased expressions of Bcl-2, Bad, and Bax in the human AD brain (Nagy and Esiri, 1997; Kitamura et al., 1998).

Fourth, the progressive and age-dependent neuronal loss observed in the Tg- β CTF99/B6 brain is an important feature of a potential AD model (Fig. 7). Moreover, the neuronal loss was detected in the Tg- β CTF99/B6 brain at 16–18 months, but not at 5 months, and the histologic evidence of this change is in agreement with the prior occurrence of behavioral changes and transcriptional or biochemical alterations, such as CB and phospho-CREB down-regulation, phospho-JNK and phospho-c-Jun up-regulation, and the altered expressions of Bcl-2 family proteins in the Tg- β CTF99/B6 brain at 14–15 months. It is likely that these biochemical alterations in advance signal the behavioral and histological pathogenesis of Tg- β CTF99/B6 mice. Neuronal loss is a central hallmark of the AD brain and eventually leads to severe or irreversible cognitive and psychiatric dysfunctions (Mattson et al., 1999). Questions such as how this prior occurrence of biochemical and histological changes specifically affects the process of neuronal loss, which factors in the aging brain critically lead to neuronal loss and behavioral impairments, what the neuronal properties of the degenerating neurons are, and what strategy is needed to delay or protect the pathophysiology of the AD-like brain can potentially be answered using this Tg- β CTF99/B6 model.

Fifth, Tg- β CTF99/B6 mice showed increased anxiety and cognitive impairments, which are the behavioral features observed in the human AD brain (Chemerinski et al., 1998; Folstein and Bylsma, 1999; Chung and Cummings, 2000; Ownby et al., 2000). Above all, the fact that these phenotypes are presented by a single transgenic line is intriguing. Although increased anxiety is a symptom of AD (Folstein and Bylsma, 1999), Tg2576 and APP23 mouse models, which are widely used in many laboratories partly because they show AD-like phenotypes such as A β -plaque deposition and cognitive deficits, do not show increased anxiety (Lalonde et al., 2002b; L-W Lee and P-L Han, unpublished observation). Thus, not all of the desirable traits mimicked by developed animal models are successfully represented by a single mouse line. With regard to this, we hope that the developed Tg- β CTF99/B6 mouse line will be a useful model for the study of the AD-like pathophysiology which underlies increased anxiety in the aging brain.

Sixth, Tg- β CTF99/B6 mice should be useful in other studies of β CTF99-related biology. Tg- β CTF99/B6 mice lead us to predict the potential toxic effects of γ -secretase inhibitor use in AD patients. As described, the genetic elimination of γ -secretase activity using a conditional knockout strategy resulted in β CTF99 accumulation in the brain and impaired learning and memory (Dewachter et al., 2002). The results of the current study strongly suggest that any AD drug that increases β CTF99 accumulation in the AD brain is likely to aggravate AD pathogenesis.

The roles of β CTF99 in AD-related pathogenesis

The observed neuronal loss and behavioral impairments of Tg- β CTF99/B6 mice raise the question as to how the transgenic β CTF99 produces such phenotypes. A growing body of evidence, albeit indirect, suggests the involvement of CTFs in AD-related pathogenesis. CTFs have been detected in tangle-bearing neurons in the AD brain (Lahiri et al., 2002), in dystrophic neurites around senile plaques (Shoji et al., 1990), and in the Down's syndrome brain (Russo et al., 2001). In cultured neuronal cells, various forms of CTFs, for examples, CTF31, AICD (CTF57 and CTF59), and β CTF99, can exert neurotoxicity, which is associated with the induction of glycogen synthase kinase 3 β or with the inhibition of histone deacetylation (Kim et al., 2003, 2004). Furthermore, the carboxyl-terminal fragment of APP with 105 amino acids (CTF105) can disturb Ca²⁺ homeostasis in cultured cells (Suh and Checler, 2002) and disrupt mitochondrial function, which leads to increased cytochrome c release and caspase 3 activation (Kim et al., 2002). In addition, CTF104 increases the production of IL-1 β , TNF α , and NO in cultured astrocytes (Suh and Checler, 2002). These molecules may contribute to neuroinflammation and cell death in the aging brain, and, although the findings of these studies are indirect, it is possible that the same mechanisms involved in these in vitro studies contribute to the pathogenic role of β CTF99 in the Tg- β CTF99/B6 brain. In this regard, the developed Tg- β CTF99/B6 mouse model could be used to dissect the in vivo role of the C-terminal fragments in AD-related pathogenesis. Tg- β CTF99/B6 mice express β CTF99(V717F), thus it is possible that histological and behavioral changes observed in Tg- β CTF99/B6 mice are due to an as-yet-unidentified toxic effect of β CTF99(V717F). Among the previously generated transgenic mouse lines expressing CTFs described in Introduction, three lines had been designed to express mutant forms of CTFs, C100(V–I) (Araki et al., 1994), C100(V–F) (Sberna et al., 1998), and

C99(I–F) (Rutten et al., 2003), although these transgenic lines do not show any obvious AD-like pathogenesis. In particular, transgenic mice expressing C100(V–F) (Sberna et al., 1998) carry a mutation essentially identical to that of Tg- β CTF99/B6 mice but showed no clear phenotype. Given the severe phenotypes shown by Tg- β CTF99/B6 mice, the absence of a phenotype in their CTF-expressing line may have been due to a low level of transgene expression or a blocking effect due to unidentified genetic backgrounds in a hybrid background. Although the Indiana mutation of APP(V717F) increases A β plaque pathogenesis, it is not known whether β CTF99(V717F) itself is more toxic than wild type β CTF99. Future studies generating additional transgenic mice expressing wild type CTF99, AICD (CTF57, CTF59), or CTF31 in the inbred C57BL/6 mice would helpfully address this and related issues.

In summary, the developed Tg- β CTF99/B6 mouse line was found to display a wide range of biological markers characterizing the AD-like brain, although Tg- β CTF99/B6 mice did not show plaque pathogenesis or tauopathy. The AD animal models described to date show the pathological and behavior features of AD to varying degrees, yet none of these lines fully captures the complete spectrum of AD symptoms, and no specific mouse line possesses all of the desirable traits of developed model animals. In this sense, the Tg- β CTF99/B6 mouse line is expected to serve as a useful AD model for the study of AD-related pathogenesis. In addition, the various biochemical, histological, and behavioral markers shown by Tg- β CTF99/B6 mice, which recapitulate the pathophysiology of the AD brain, should provide a useful means of developing drugs aimed at treating and delaying the expression of AD symptoms.

Acknowledgment

This work was supported by a grant (M103KV010020 03K2201 02020) from Brain Research Center, The 21st Century Frontier Research Program of the Ministry of Science and Technology, Republic of Korea.

Appendix A. Supplementary data

Supplementary data associated with this article can be found in the online version at [doi:10.1016/j.nbd.2005.09.011](https://doi.org/10.1016/j.nbd.2005.09.011).

References

- Araki, E., Yamada, T., Takemura, K., Yamaguchi, H., Sakimura, K., et al., 1994. Transgenic mice expressing the amyloid β protein-containing carboxyl-terminal fragment of the Alzheimer's amyloid precursor protein. *Int. J. Exp. Clin. Invest.* 2, 100–106.
- Barrot, M., Olivier, J.D., Perrotti, L.I., DiLeone, R.J., Berton, O., et al., 2002. CREB activity in the nucleus accumbens shell controls gating of behavioral responses to emotional stimuli. *Proc. Natl. Acad. Sci. U. S. A.* 99, 11435–11440.
- Berger-Sweeney, J., McPhie, D.L., Arters, J.A., Greenan, J., Oster-Granite, M.L., Neve, R.L., 1999. Impairments in learning and memory accompanied by neurodegeneration in mice transgenic for the carboxyl-terminus of the amyloid precursor protein. *Brain Res. Mol. Brain Res.* 66, 150–162.
- Berridge, M.J., 1998. Neuronal calcium signaling. *Neuron* 21, 13–26.
- Blendy, J.A., Kaestner, K.H., Schmid, W., Gass, P., Schutz, G., 1996. Targeting of the CREB gene leads to up-regulation of a novel CREB mRNA isoform. *EMBO J.* 15, 1098–1106.
- Bourtchuladze, R., Frenguelli, B., Blendy, J., Cioffi, D., Schutz, G., Silva, A.J., 1994. Deficient long-term memory in mice with a targeted mutation of the cAMP-responsive element-binding protein. *Cell* 79, 59–68.
- Bu, J., Sathyendra, V., Nagykerly, N., Geula, C., 2003. Age-related changes in calbindin-D28k, calretinin, and parvalbumin-immunoreactive neurons in the human cerebral cortex. *Exp. Neurol.* 182, 220–231.
- Carafoli, E., 2002. Calcium signaling: a tale for all seasons. *Proc. Natl. Acad. Sci. U. S. A.* 99, 1115–1122.
- Che, Y., Piao, C.S., Han, P.-L., Lee, J.-K., 2001. Delayed induction of aB-crystallin in activated glia cells of hippocampus in KA-treated mouse brain. *J. Neurosci. Res.* 65, 425–431.
- Chemmerinski, E., Petracca, G., Manes, F., Leiguarda, R., Starkstein, S.E., 1998. Prevalence and correlates of anxiety in Alzheimer's disease. *Depress. Anxiety* 7, 166–170.
- Chung, J.A., Cummings, J.L., 2000. Neurobehavioral and neuropsychiatric symptoms in Alzheimer's disease: characteristics and treatment. *Neurol. Clin.* 18, 829–846.
- Colombo, P.J., Brightwell, J.J., Countryman, R.A., 2003. Cognitive strategy-specific increases in phosphorylated cAMP response element-binding protein and c-Fos in the hippocampus and dorsal striatum. *J. Neurosci.* 23, 3547–3554.
- Davies, A.M., 1995. The Bcl-2 family of proteins, and the regulation of neuronal survival. *Trends Neurosci.* 18, 355–358.
- Dewachter, I., Reverse, D., Caluwaerts, N., Ris, L., Kuiperi, C., et al., 2002. Neuronal deficiency of presenilin 1 inhibits amyloid plaque formation and corrects hippocampal long-term potentiation but not a cognitive defect of amyloid precursor protein [V717I] transgenic mice. *J. Neurosci.* 22, 3445–3453.
- Esler, W.P., Wolfe, M.S., 2001. A portrait of Alzheimer secretases—New features and familiar faces. *Science* 293, 1449–1454.
- Franklin, K.B.J., Paxinos, P., 1997. *The Mouse Brain in Stereotaxic Coordinates*. Academic Press, San Diego.
- Folstein, M.F., Bylsma, F.W., 1999. Noncognitive symptoms of Alzheimer Disease. In: Terry (Ed.), *Alzheimer Disease*, 2nd ed. Lippincott Williams and Wilkins, Philadelphia.
- Fukuchi, K., Ho, L., Younkin, S.G., Kunkel, D.D., Ogburn, C.E., et al., 1996. High levels of circulating beta-amyloid peptide do not cause cerebral beta-amyloidosis in transgenic mice. *Am. J. Pathol.* 149, 219–227.
- Games, D., Adams, D., Alessandrini, R., Barbour, R., Berthelette, P., et al., 1995. Alzheimer-type neuropathology in transgenic mice overexpressing V717F beta-amyloid precursor protein. *Nature* 373, 523–527.
- Gervais, F.G., Xu, D., Robertson, G.S., Vaillancourt, J.P., Zhu, Y., et al., 1999. Involvement of caspases in proteolytic cleavage of Alzheimer's amyloid-beta precursor protein and amyloidogenic A beta peptide formation. *Cell* 97, 395–406.
- Guzowski, J.F., McGaugh, J.L., 1997. Antisense oligodeoxynucleotide-mediated disruption of hippocampal cAMP response element binding protein levels impairs consolidation of memory for water maze training. *Proc. Natl. Acad. Sci. U. S. A.* 94, 2693–2698.
- Hsiao, K., Chapman, P., Nilsen, S., Eckman, C., Harigaya, Y., et al., 1996. Correlative memory deficits, A β elevation, and amyloid plaques in transgenic mice. *Science* 274, 99–102.
- Horgan, B., Beddington, R., Costantini, F., Lacy, E., 1994. *Manipulating the Mouse Embryos. A Laboratory Manual*. 2nd ed. Cold Spring Harbor Press.
- Iacopino, A.M., Christakos, S., 1990. Specific reduction of calcium-binding protein (28-kilodalton calbindin-D) gene expression in aging and neurodegenerative diseases. *Proc. Natl. Acad. Sci. U. S. A.* 87, 4078–4082.
- Irizarry, M.C., Soriano, F., McNamara, M., Page, K.J., Schenk, D., et al., 1997. A β deposition is associated with neuropil changes, but not

- with overt neuronal loss in the human amyloid precursor protein V717F (PDAPP) transgenic mouse. *J. Neurosci.* 17, 7053–7059.
- Josselyn, S.A., Shi, C., Carlezon, W.A., Neve, R.L., Nestler, E.J., Davis, M., 2001. Long-term memory is facilitated by cAMP response element-binding protein overexpression in the amygdala. *J. Neurosci.* 21, 2404–2412.
- Kammesheidt, A., Boyce, F.M., Spanoyannis, A.F., Cummings, B.J., Ortegón, M., et al., 1992. Deposition of beta/A4 immunoreactivity and neuronal pathology in transgenic mice expressing the carboxyl-terminal fragment of the Alzheimer amyloid precursor in the brain. *Proc. Natl. Acad. Sci. U. S. A.* 89, 10857–10861.
- Kim, H.S., Lee, J.H., Lee, J.P., Kim, E.M., Chang, K.A., et al., 2002. Amyloid beta peptide induces cytochrome C release from isolated mitochondria. *NeuroReport* 13, 1989–1993.
- Kim, H.S., Kim, E.M., Lee, J.P., Park, C.H., Kim, S., et al., 2003. C-terminal fragments of amyloid precursor protein exert neurotoxicity by inducing glycogen synthase kinase-3beta expression. *FASEB J.* 17, 1951–1953.
- Kim, H.S., Kim, E.M., Kim, N.J., Chang, K.A., Choi, Y., et al., 2004. Inhibition of histone deacetylation enhances the neurotoxicity induced by the C-terminal fragments of amyloid precursor protein. *J. Neurosci. Res.* 75, 117–124.
- Kitamura, Y., Shimohama, S., Kamoshima, W., Ota, T., Matsuoka, Y., et al., 1998. Alteration of proteins regulating apoptosis, Bcl-2, Bcl-x, Bax, Bak, Bad, ICH-1 and CPP32, in Alzheimer's disease. *Brain Res.* 780, 260–269.
- Lahiri, D.K., Kotwal, G.J., Farlow, M.R., Sima, A., Kupsky, W., et al., 2002. The role of the carboxyl-terminal fragments of amyloid precursor protein in Alzheimer's disease. *Ann. N. Y. Acad. Sci.* 973, 334–339.
- Lalonde, R., Dumont, M., Fukuchi, K., Strazille, C., 2002a. Transgenic mice expressing the human C99 terminal fragment of betaAPP: effects on spatial learning, exploration, anxiety, and motor coordination. *Exp. Gerontol.* 37, 1399–1410.
- Lalonde, R., Dumont, M., Staufienbiel, M., Sturchler-Pierrat, C., Strazielle, C., 2002b. Spatial learning, exploration, anxiety, and motor coordination in female APP23 transgenic mice with the Swedish mutation. *Brain Res.* 956, 36–44.
- Lee, J.Y., Mook-Jung, I., Koh, J.Y., 1999. Histochemically reactive zinc in plaques of the Swedish mutant beta-amyloid precursor protein transgenic mice. *J. Neurosci.* RC10, 1–5.
- Lee, K.W., Hong, J.H., Choi, I.Y., Che, Y., Lee, J.K., et al., 2002. Impaired D2 dopamine receptor function in mice lacking type 5 adenylyl cyclase. *J. Neurosci.* 15, 7931–7940.
- Lee, K.-W., Lee, S.H., Kim, H., Song, J.-S., Yang, S.-D., et al., 2004. Progressive cognitive impairment and anxiety induction in the absence of plaque deposition in C57BL/6 inbred mice expressing transgenic amyloid precursor protein. *J. Neurosci. Res.* 76, 572–580.
- Leuba, G., Kraftsik, R., Saini, K., 1998. Quantitative distribution of parvalbumin, calretinin, and calbindin D-28k immunoreactive neurons in the visual cortex of normal and Alzheimer cases. *Exp. Neurol.* 152, 278–291.
- Li, Q.X., Maynard, C., Cappai, R., McLean, C.A., Cherny, R.A., et al., 1999. Intracellular accumulation of detergent-soluble amyloidogenic A beta fragment of Alzheimer's disease precursor protein in the hippocampus of aged transgenic mice. *J. Neurochem.* 72, 2479–2487.
- Li, Y.M., Xu, M., Lai, M.T., Huang, Q., Castro, J.L., et al., 2000. Photoactivated gamma-secretase inhibitors directed to the active site covalently label presenilin 1. *Nature* 405, 689–694.
- Lu, D.C., Rabizadeh, S., Chandra, S., Shayya, R.F., Ellerby, L.M., et al., 2000. A second cytotoxic proteolytic peptide derived from amyloid beta-protein precursor. *Nat. Med.* 6, 397–404.
- Marambaud, P., Wen, P.H., Dutt, A., Shioi, J., Takashima, A., et al., 2003. A CBP binding transcriptional repressor produced by the PS1/epsilon-cleavage of N-cadherin is inhibited by PS1 FAD mutations. *Cell* 114, 635–645.
- Mattson, M.P., 1998. Modification of ion homeostasis by lipid peroxidation: roles in neuronal degeneration and adaptive plasticity. *Trends Neurosci.* 21, 53–57.
- Mattson, M.P., Rydel, R.E., Lieberburg, I., Smith-Swintosky, V.L., 1993. Altered calcium signaling and neuronal injury: stroke and Alzheimer's disease as examples. *Ann. N. Y. Acad. Sci.* 679, 1–21.
- Mattson, M.P., Pedersen, W.A., Duan, W., Culmsee, C., Camandola, S., 1999. Cellular and molecular mechanisms underlying perturbed energy metabolism and neuronal degeneration in Alzheimer's and Parkinson's diseases. *Ann. N. Y. Acad. Sci.* 893, 154–175.
- Mayford, M., Kandel, E.R., 1999. Genetic approaches to memory storage. *Trends Genet.* 15, 463–470.
- Mikkonen, M., Alafuzoff, I., Tapiola, T., Soininen, H., Miettinen, R., 1999. Subfield- and layer-specific changes in parvalbumin, calretinin and calbindin-D28K immunoreactivity in the entorhinal cortex in Alzheimer's disease. *Neuroscience* 92, 515–532.
- Molinari, S., Battini, R., Ferrari, S., Pozzi, L., Killcross, A.S., et al., 1996. Deficits in memory and hippocampal long-term potentiation in mice with reduced calbindin D28K expression. *Proc. Natl. Acad. Sci. U. S. A.* 93, 8028–8033.
- Nagy, Z.S., Esiri, M.M., 1997. Apoptosis-related protein expression in the hippocampus in Alzheimer's disease. *Neurobiol. Aging* 18, 565–571.
- Nalbantoglu, J., Tirado-Santiago, G., Lahsaini, A., Poirier, J., Goncalves, O., et al., 1997. Impaired learning and LTP in mice expressing the carboxy terminus of the Alzheimer amyloid precursor protein. *Science* 387, 500–505.
- Naruse, S., Thinakaran, G., Luo, J.J., Kusiak, J.W., Tomita, T., et al., 1998. Effects of PS1 deficiency on membrane protein trafficking in neurons. *Neuron* 21, 1213–1221.
- Neve, R.L., Boyce, F.M., McPhie, D.L., Greenan, J., Oster-Granite, M.L., 1996. Transgenic mice expressing APP-C100 in the brain. *Neurobiol. Aging* 17, 191–203.
- Oster-Granite, M.L., McPhie, D.L., Greenan, J., Neve, R.L., 1996. Age-dependent neuronal and synaptic degeneration in mice transgenic for the C terminus of the amyloid precursor protein. *J. Neurosci.* 16, 6732–6741.
- Ownby, R.L., Harwood, D.G., Barker, W.W., Duara, R., 2000. Predictors of anxiety in patients with Alzheimer's disease. *Depress. Anxiety* 11, 38–42.
- Palop, J.J., Jones, B., Kekonius, L., Chin, J., Yu, G.Q., et al., 2003. Neuronal depletion of calcium-dependent proteins in the dentate gyrus is tightly linked to Alzheimer's disease-related cognitive deficits. *J. Neurosci.* 100, 9572–9577.
- Rodgers, R.J., Dalvi, A., 1997. Anxiety, defense and the elevated plus-maze. *Neurosci. Biobehav. Rev.* 21, 801–810.
- Russo, C., Salis, S., Dolcini, V., Venezia, V., Song, X.H., et al., 2001. Amino-terminal modification and tyrosine phosphorylation of carboxy-terminal fragments of the amyloid precursor protein in Alzheimer's disease and Down's syndrome brain. *Neurobiol. Dis.* 8, 173–180.
- Rutten, B.P., Wirths, O., Van de Berg, W.D., Lichtenthaler, S.F., Vehoff, J., et al., 2003. No alterations of hippocampal neuronal number and synaptic bouton number in a transgenic mouse model expressing the beta-cleaved C-terminal APP fragment. *Neurobiol. Dis.* 12, 110–120.
- Sandhu, F.A., Salim, M., Zain, S.B., 1991. Expression of the human beta-amyloid protein of Alzheimer's disease specifically in the brains of transgenic mice. *J. Biol. Chem.* 266, 21331–21334.
- Sasahara, M., Fries, J.W., Raines, E.W., Gown, A.M., Westrum, L.E., et al., 1991. PDGF B-chain in neurons of the central nervous system, posterior pituitary, and in a transgenic model. *Cell* 64, 217–227.
- Sato, M., Kawarabayashi, T., Shoji, M., Kobayashi, T., Tada, N., et al., 1997. Neurodegeneration and gliosis in transgenic mice overexpressing a carboxy-terminal fragment of Alzheimer amyloid-beta protein precursor. *Dementia Geriatr. Cognit. Disord.* 8, 296–307.
- Savage, M.J., Lin, Y.G., Ciallella, J.R., Flood, D.G., Scott, R.W., 2002. Activation of c-Jun N-terminal kinase and p38 in an Alzheimer's disease model is associated with amyloid deposition. *J. Neurosci.* 22, 3376–3385.

- Sberna, G., Saez-Valero, J., Li, Q.X., Czech, C., Beyreuther, K., et al., 1998. Acetylcholinesterase is increased in the brains of transgenic mice expressing the C-terminal fragment (CT100) of the beta-amyloid protein precursor of Alzheimer's disease. *J. Neurochem.* 71, 723–731.
- Shoji, M., Hirai, S., Yamaguchi, H., Harigaya, Y., Kawarabayashi, T., 1990. Amyloid beta-protein precursor accumulates in dystrophic neurites of senile plaques in Alzheimer-type dementia. *Brain Res.* 512, 164–168.
- Song, W., Nadeau, P., Yuan, M., Yang, X., Shen, J., Yankner, B.A., 1999. Proteolytic release and nuclear translocation of Notch-1 are induced by presenilin-1 and impaired by pathogenic presenilin-1 mutations. *Proc. Natl. Acad. Sci. U. S. A.* 96, 6959–6963.
- Steiner, H., Capell, A., Leimer, U., Haass, C., 1999. Genes and mechanisms involved in beta-amyloid generation and Alzheimer's disease. *Eur. Arch. Psychiat. Clin. Neurosci.* 249, 266–270.
- Suh, Y.H., Checler, F., 2002. Amyloid precursor protein, presenilins, and alpha-synuclein: molecular pathogenesis and pharmacological applications in Alzheimer's disease. *Pharmacol. Rev.* 54, 469–525.
- Viola, H., Furman, M., Izquierdo, L.A., Alonso, M., Barros, D.M., et al., 2000. Phosphorylated cAMP response element-binding protein as a molecular marker of memory processing in rat hippocampus: effect of novelty. *J. Neurosci.* 20, RC112.
- Wong, P.C., Zheng, H., Chen, H., Becher, M.W., Sirinathsinghji, D.J., et al., 1997. Presenilin 1 is required for Notch1 and DIII expression in the paraxial mesoderm. *Nature* 387, 288–292.
- Yamamoto-Sasaki, M., Ozawa, H., Saito, T., Rosler, M., Riederer, P., 1999. Impaired phosphorylation of cyclic AMP response element binding protein in the hippocampus of dementia of the Alzheimer type. *Brain Res.* 824, 300–303.
- Yu, C., Kim, S.H., Ikeuchi, T., Xu, H., Gasparini, L., et al., 2001a. Characterization of a presenilin-mediated amyloid precursor protein carboxyl-terminal fragment gamma. Evidence for distinct mechanisms involved in gamma-secretase processing of the APP and Notch1 transmembrane domains. *J. Biol. Chem.* 276, 43756–43760.
- Yu, H., Saura, C.A., Choi, S.Y., Sun, L.D., Yang, X., et al., 2001b. APP processing and synaptic plasticity in presenilin-1 conditional knockout mice. *Neuron* 31, 713–726.
- Wall, P.M., Messier, C., 2001. Methodological and conceptual issues in the use of the elevated plus-maze as a psychological measurement instrument of animal anxiety-like behavior. *Neurosci. Biobehav. Rev.* 25, 275–286.
- Xia, W., Zhang, J., Ostaszewski, B.L., Kimberly, W.T., et al., 1998. Presenilin 1 regulates the processing of beta-amyloid precursor protein C-terminal fragments and the generation of amyloid beta-protein in endoplasmic reticulum and Golgi. *Biochemistry* 37, 16465–16471.
- Zhu, X., Raina, A.K., Rottkamp, C.A., Aliev, G., Perry, G., 2001. Activation and redistribution of *c-jun* N-terminal kinase/stress activated protein kinase in degenerating neurons in Alzheimer's disease. *J. Neurochem.* 76, 435–441.